HAL
open science

Direct measurement of spatial modes of a micro-cantilever from thermal noise

Pierdomenico Paolino, Bruno Tiribilli, Ludovic Bellon

To cite this version:

Pierdomenico Paolino, Bruno Tiribilli, Ludovic Bellon. Direct measurement of spatial modes of a micro-cantilever from thermal noise. 2009. ensl-00379365v1

HAL Id: ensl-00379365

https://ens-lyon.hal.science/ensl-00379365v1

Preprint submitted on 28 Apr 2009 (v1), last revised 16 Nov 2009 (v4)

HAL is a multi-disciplinary open access archive for the deposit and dissemination of scientific research documents, whether they are published or not. The documents may come from teaching and research institutions in France or abroad, or from public or private research centers.

L'archive ouverte pluridisciplinaire **HAL**, est destinée au dépôt et à la diffusion de documents scientifiques de niveau recherche, publiés ou non, émanant des établissements d'enseignement et de recherche français ou étrangers, des laboratoires publics ou privés.

Direct measurement of spatial modes of a micro-cantilever from thermal noise

Pierdomenico Paolino*
Université de Lyon, Laboratoire de physique, École Normale Supérieure de Lyon
CNRS UMR 5672, Lyon, France
Bruno Tiribilli
Istituto dei Sistemi Complessi, Consiglio Nazionale delle Ricerche, Sesto Fiorentino
Firenze, Italy
Ludovic Bellon†
Université de Lyon, Laboratoire de physique, École Normale Supérieure de Lyon
CNRS UMR 5672, Lyon, France

(submitted to Applied Physics Letter on April 28, 2009)

Abstract

Measurements of the deflection induced by the thermal noise have been performed on a rectangular AFM cantilever in air. The detection method, based on polarization interferometry, can achieve a resolution of $10^{-14}\,\mathrm{m}/\sqrt{\mathrm{Hz}}$ in the frequency range $1\,\mathrm{kHz} - 800\,\mathrm{kHz}$. The focused beam from the interferometer probes the cantilever at different position along its length and the spatial modes shapes are determined up to the 4th resonance, without external excitation. Results are in good agreement with theoretically expected behavior. From the thermal noise spectrum accurate determination of the elastic constant of the cantilever is also achieved.

*present address: Université de Lyon, LTDS, École Centrale Lyon, CNRS UMR 5513, Ecully, France
†corresponding author : ludovic.bellon@ens-lyon.fr

Atomic force microscopy (AFM) is currently used in a great variety of studies involving small forces measurement [1] including unfolding of protein [2, 3], probing the structure of biological membranes [4] and monitoring the mechanical response of living cells [5, 6] as well as MEMS and other nanotechnological devices [7, 8].

All those applications exploit the great accuracy in measuring the cantilever deflection offered by AFM and convert this measure to unit of force assuming the cantilever as a spring with known elastic constant. The manufacturer often specify the spring constant of their cantilever in a wide range of values, mainly because of the great uncertainties in the dimensions, particularly the thickness, resulting from the fabrication process. To overcome this problem several techniques have been proposed to calibrate cantilever spring constant [1, 9, 10, 11, 12]. The reader is referred to the work of Burnham and co-workers [13] and the references therein for comparative summary of the different techniques.

One of the first and still most commonly used is the so called thermal calibration method [11] based on the measurement of the vibration amplitude of the free end of a cantilever exited by thermal noise. The first resonance of the thermal noise spectrum is related back to the spring constant of the cantilever modeled as an harmonic oscillator. In a more accurate model, Butt and Jaschke [14] introduced a correction factor deduced from the Euler-Bernoulli description of the flexural dynamic of a free-clamped beam.

In this work we measure the first four modes of the vibration amplitude due to the thermal noise and compare the rms amplitude spatial distribution with the eigenmode of the Euler-Bernoulli model. Furthermore, we present an extention of the thermal calibration method for the spring constant based on the multi-mode measurement.

Let us first recall the main lines of Butt and Jaschke's work to interpret our measurements. The cantilever is sketched on Fig. 1. Its length L is supposed to be much larger than its width W, which itself is much larger than its thickness T. We will limit ourself in this study to the flexural modes of the cantilever: the deformations are supposed to be only perpendicular to its length (along axis z of Fig. 1) and uniform across its width. Theses deformation can thus be described by the deflection $d(x,t)$, x being the spacial coordinate along the beam, and t the time. The generic solution of the Euler-Bernoulli equation can be expressed as follows:

$$d(x,t) = \sum_{n=1}^{\infty} d_n(t)\phi_n\left(\frac{x}{L}\right) \tag{1}$$

in which the spatial solutions are in the form

$$\phi_n\left(\frac{x}{L}\right) = \left[\cos\left(\alpha_n\frac{x}{L}\right) - \cosh\left(\alpha_n\frac{x}{L}\right)\right] - \frac{\cos(\alpha_n)+\cosh(\alpha_n)}{\sin(\alpha_n)+\sinh(\alpha_n)}\left[\sin\left(\alpha_n\frac{x}{L}\right) - \sinh\left(\alpha_n\frac{x}{L}\right)\right] \tag{2}$$

where the α_n satisfy the relation

$$1 + \cos(\alpha_n)\cosh(\alpha_n) = 0 \tag{3}$$

which leads to $\alpha_1 = 1.875$, $\alpha_2 = 4.694$, $\ldots$, $\alpha_n \approx (n-1/2)\pi$. The amplitude $d_n(t)$ of each modes are governed by harmonic oscillator equations, with stiffness k_n, mass m and resonance frequencies f_n:

$$k_n = \frac{\alpha_n^4}{3}k_c = \frac{\alpha_n^4}{3}\frac{EWT^3}{4L^3} \tag{4}$$

$$m = m_c = \rho LWT \tag{5}$$

$$f_n = \frac{1}{2\pi}\sqrt{\frac{k_n}{m}} \tag{6}$$

where k_c and m_c are the static stiffness and mass of the cantilever, and E and ρ are the young modulus and density of its material.

We furthermore consider, under the hypothesis of thermal equilibrium, that the thermal noise driven deflection follows the equipartition theorem and each resonance mode can be considered as an independent harmonic oscillator [14] with mean quadratic fluctuations $\langle d_n^2\rangle$:

$$\frac{1}{2}k_BT = \frac{1}{2}k_n\langle d_n^2\rangle \tag{7}$$

where $\langle\ \rangle$ represent time average.

In our experiment, we will measure both the amplitude of the thermal noise distibution among the modes $\langle d_n^2\rangle$ and their spatial shape $\phi_n(x/L)$.

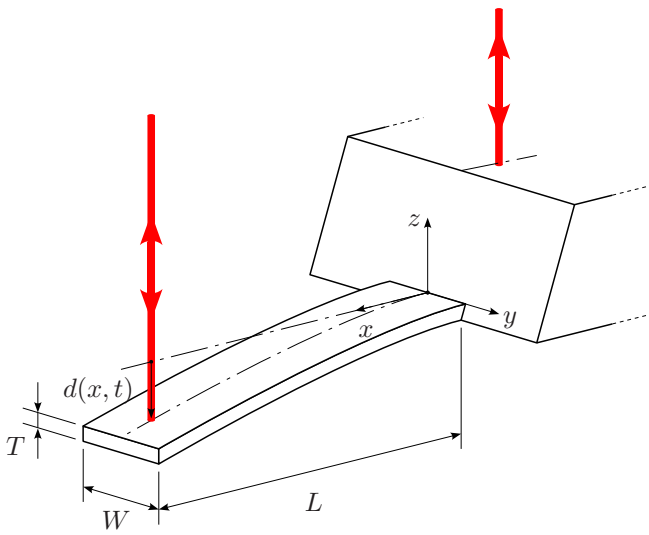

Figure 1: The thermal fluctuations of deflexion $d(x,t)$ of a rectangular cantilever (BS-Cont-GB-G) are measured with a differential interferometer : the optical path difference between the reference beam, reflecting on the chip holding the cantilever, and the sensing beam, focused on the cantilever, directly gives a calibrated measurement of spatially resolved deflexion [15]. The whole cantilever can be probed by displacing the beams along its length. Notations used in the text are reported on the figure.

We use gold coated BudgetSensors Atomic Force Microscopy (AFM) cantilevers (Cont-GB-G). They present a nominal rectangular geometry: $L = 450\,\mu$m long, $W = 50\,\mu$m wide and $T = 2\,\mu$m thick, with a 70 nm gold layer on both sides. We observe the fluctuation of the cantilever deflection induced by thermal noise. The measurement is performed with a home made interferometric deflection sensor [15, 16], inspired by the original design of Schonenberger [17] with a quadrature phase detection technique [18]: the interference between the reference laser beam reflecting on the chip of the cantilever [15] and the sensing beam on the cantilever gives a direct measurement of the deflection $d(x,t)$, with very high accuracy (see Fig. 1). A first advantage of the technique is that it offers a calibrated measurement of deflection, without conversion factor from angle to displacement, as in the standard optical lever technique common in AFM. A second advantage of our detection system is a very low intrinsic noise, as illustrated in Fig. 2 with the power spectrum density of a rigid mirror (bottom black line): the light intensities on the photo diodes are tuned exactly as during the measurement on the cantilever, but since the mirror is still the measured spectrum reflects only the detection noise. This background noise is as low as $3 \times 10^{-28}\,\mathrm{m}^2/\mathrm{Hz}$, in the frequency range from 1 kHz to 800 kHz, just 10 % higher than the shot noise limit of our detection system. A third advantage is that the precision of the measurement is independent of the focused beam size on the cantilever, which was tuned as small as $10\,\mu$m to ensure good spatial resolution of the measurement.

When translating the focusing lens with respect to the cantilever, both reference and sensing laser beams are shifted along the chip and cantilever respectively [15]. The chip first structural mode is at very high frequency compared to that of the cantilever, hence it is considered as a rigid fixed mirror independently of the actual reference beam position on top of it. The measured interference signal is therefore only due to the thermal noise driven deflection of the cantilever. Fig. 2 illustrates such a spectrum when the sensing beam is close to the free end. The signal to noise ratio is enough to identify the first four flexural resonances (as well as the first two torsional resonances, that are visible due to an approximate centering of the spot laterally). The peak frequencies are positioned according to the relation that directly derive from equations 4 and 6:

$$\frac{f_n}{f_1} = \frac{\alpha_n^2}{\alpha_1^2} \tag{8}$$

The experimental ratios of resonance frequencies are in good agreement with the expected values of the coefficients (table 1).

A precision screw allows adjusting the horizontal position of the focusing lens and locate the sensing beam at different positions along the cantilever length while the reference beam is always on the chip [15]. For each measurement, the x position of the laser spot on the cantilever can be estimated from the image acquired

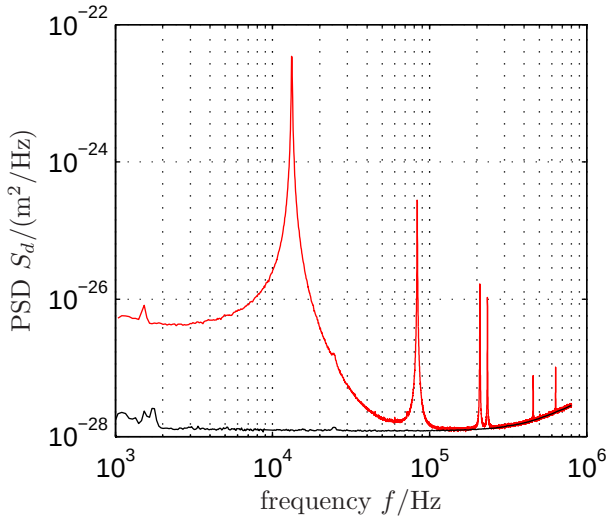

Figure 2: Power Spectrum Density (PSD) S_d of thermal noise induced deflexion (red curve) measured close to the free end of the cantilever as a function of frequency f (log scale on both axis). The first 4 flexural modes and first 2 torsional modes are clearly above the background noise (bottom black line), measured with a rigid mirror. With our interferometric setup, resolution better than $1.7 \times 10^{-14}\,\mathrm{m}/\sqrt{\mathrm{Hz}}$ can be achieve on the whole frequency range explored here (1 kHz – 800 kHz).

by a simple CCD camera. The spot center in the images can be detected with about $\pm 1.4\,\mu$m accuracy on the cantilever. Measurement have been repeated at about 15 μm steps. At every position we measure the deflection $d(x,t)$ produced by thermal excitation of the cantilever and evaluate the Power Spectrum Density (PSD) $S_d(x,f)$. The complete set of results is reported in Fig. 3 as a 3D representation. The first four oscillation modes can be clearly seen with their respective number of nodes. Two further peaks can be noted, the first at about 220 kHz and a second, of smaller amplitude, at 790 kHz, that we can attribute to the first and second torsional modes.

For a quantitative characterization of the mode shape we determine the rms amplitude of each mode $\langle \delta_n^2(x) \rangle$ as a function of the position x. To this aim we integrated the PSD in a convenient frequency interval $2\Delta f$ around each peak:

$$\langle \delta_n^2(x) \rangle = \int_{f_n-\Delta f}^{f_n+\Delta f} S_d(x,f)df \tag{9}$$

According to equation 1, we should have

$$\langle \delta_n^2(x) \rangle = \langle d_n^2 \rangle \left| \phi_n \left(\frac{x}{L} \right) \right|^2 \tag{10}$$

It is then possible to fit the data with the expression of $\langle d_n^2 \rangle$ (equation 7) with 3 free parameters: the length of the lever L', the clamping position x_0 and the static spring constant of the cantilever k'_c. We realize the fit on the rms amplitude *simultaneously* on the 4 modes with the following functions:

$$\sqrt{\langle \delta_n^2(x) \rangle} = \sqrt{\frac{4}{\alpha_n^4} \frac{k_B T}{k'_c}} \left| \phi_n \left(\frac{x - x_0}{L'} \right) \right| \tag{11}$$

where $n = 1, ..., 4$. The red curves in Fig. 4 represent the result of the fit on the four considered modes, in good agreement for all modes. The best fit values are: $L' = 450\,\mu$m and $k'_c = 0.37\,$N/m. The length and stiffness are compatible with the values provided by the manufacturer ($L = (450 \pm 10)\mu m$ and k_c from 0.07 N/m to 0.4 N/m).

It's worth noting that the accuracy of our instrument provides a precise measurement of the thermal noise driven deflection along the cantilever length and allows to verify the Euler-Bernoulli model for the micro-lever. Furthermore this multi-mode approach provide a more reliable way to estimate the elastic constant of a cantilever

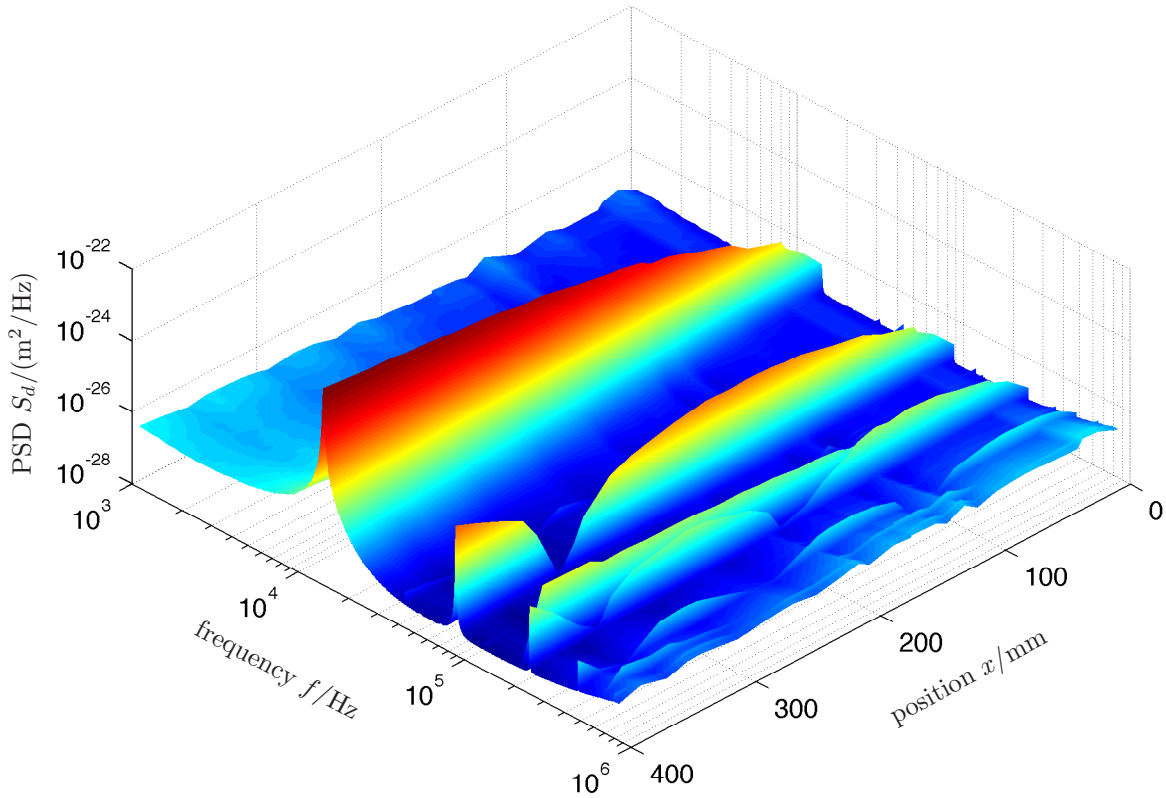

Figure 3: Power Spectrum Density (PSD) S_d of thermal noise induced deflexion as a function of position x along the cantilever and frequency f. The first 4 normal modes are clearly visible, with a vanishing amplitude toward the clamped extremity of the mechanical beam and the nodes of each mode. Another vibration peak with no nodes is also visible close to the third mode, it is attributed to the first mode in torsion, but is not studied in this letter.

with respect to the standard thermal noise calibration method limited to the integral of the first mode only and just at the cantilever free end (circled point in Fig. 4). Actually a precise measurement of the cantilever stiffness could be obtained from the first 3 modes only, the presence of the nodes providing a favorable constrain to the fitting process.

Experimental PSD curves show peaks width depending on the viscosity of the environment, mainly due to the viscous drag of the fluid, an effect that is not considered in the Euler-Bernoulli framework. A simple model that account for this aspect, for each eigenmode, is a damped harmonic oscillator characterized by three parameter: the resonance frequency f_n, the elastic constant k_n and the quality factor Q_n. The PSD of the damped oscillator can be expressed as:

$$S_d(f) = \frac{2k_BT}{k_n\pi f_n}\frac{Q_n}{(1-u^2)^2Q_n^2+u^2} \tag{12}$$

with $u = f/f_n$ the normalised frequency. For each mode the PSD depends on the spatial coordinate along the cantilever length still according to $|\phi_n(x)|^2$. The Q_n are evaluated from experimental data by a fitting in the region around the peaks of each node (see Fig. 5). Those values are constant along the cantilever. Since the elastic constant k_n and resonant frequency f_n of each mode is known, quality factor Q_n is the only free parameter in the fit. In table 1 the Q_n values of the first four modes are compared with the hydrodynamic predictions of the Sader model [19] that account for viscous effect in the fluid. These predictions were computed with tabulated values of silicon and gold for the Young modulus and density, and the physical dimensions of the cantilever (length, width and thickness) were tuned within the manufacturer tolerance to match the experimental observation. Note that the elastic modulus of gold and silicon are of the same order of magnitude, whereas the density of gold is about eight times that of silicon, therefore even a thin coating layer of 70 nm produces a mass increment of about 60% that cannot be neglected in the evaluation of total mass.

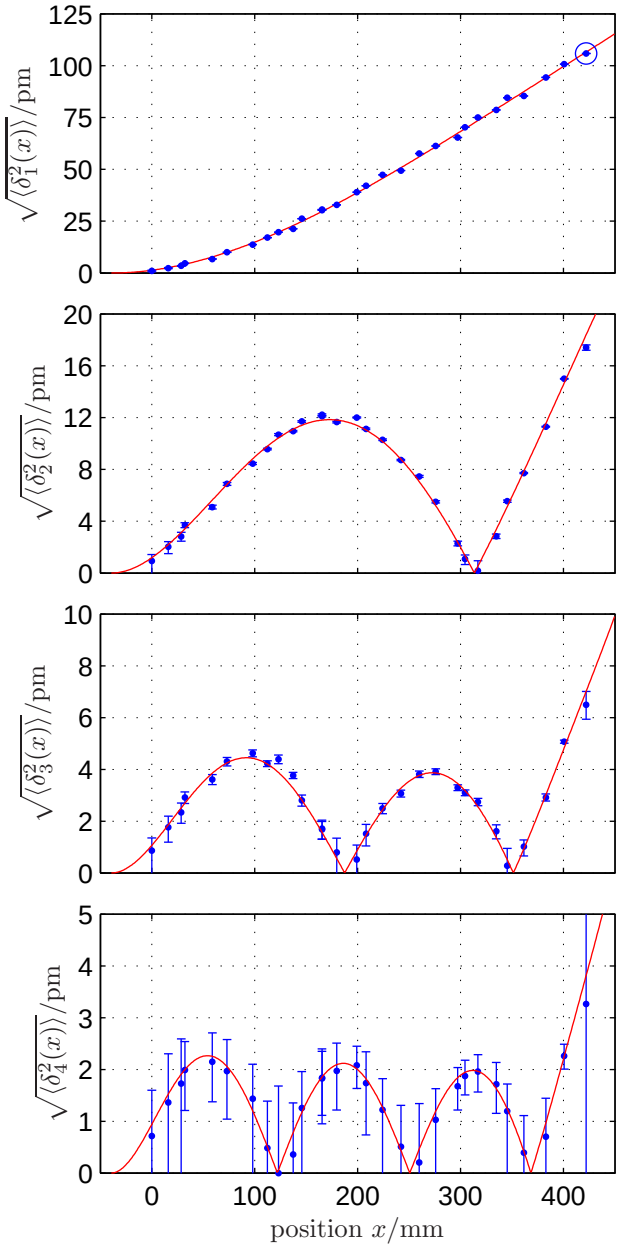

Figure 4: Amplitude of thermal noise for the first 4 flexural modes along the cantilever. Errors bars correspond to the equivalent noise of the detection system in the bandwidth chosen around each resonance (a very conservative estimation of incertitude). The simultaneous fit (red curves) of the 4 resonances with the normal modes shapes is excellent and leads to a precise measurement of the stiffness of the cantilever. The common calibration method for the spring constant considers only the value of $\delta_1^2(L)$, the circled point in the upper graph.

Mode	f_n/kHz	f_n/f_1	α_n^2/α_1^2	Q_n	Q_n^{Sader}
1	14.046	1	1	88	85
2	87.921	6.26	6.27	231	243
3	245.500	17.48	17.55	420	423
4	479.970	34.17	34.40	680	601

Table 1: measured and expected parameters for first 4 flexural modes

A good agreement between the model and experiment is observed for the first three resonances, but at the highest frequency a deviation is observed: a lower dissipation than that foreseen by the Sader model. This behavior was already observed by Maali et al [20].

This deviation is expected since the original Sader model neglects the 3D nature of the fluid flowing around the cantilever, an effect increasing with mode number [19]. In an extended model by Sader and co-workers [21], such a correction is also observed in the same direction as in our observation.

We presented in this paper a high precision measurement of thermal noise induced deflexion of a soft rectangular micro-cantilever as a function of frequency and position along the mechanical beam. The 4 first flexural spatial modes could be studied without any external forcing. Their shapes are very well fitted by the Euler-Bernoulli model, and their vibration amplitudes accurately described in the Butt and Jaschke [14] framework. Furthermore this multi-mode approach provides a extension of the standard thermal noise calibration method for the spring constant of the cantilever, with a more robust estimation: it is obtained by a simultaneous fit on several modes, when the classic measurement is limited to the integral of the first mode only and just at the cantilever free end. Quality factors of resonances are also robustly extracted from the measurements and compare well to the Sader estimation [19].

Although presented here on an academic geometry, this method could be applied to more complex structures, such as double clamped beams, membranes and other micromechanical structures. The absence of external forcing (that may not be well controlled or hard to characterize) and the great resolution of the interferometric setup make it a very promising tool for the mechanical characterization of MEMS.

Acknowledgements The authors thank F. Vittoz and F. Ropars for technical support, and S. Ciliberto, A. Petrosyan and J.P. Aimé for stimulating discussions. One of us (B.T.) thanks École Normale Supérieure de Lyon for invited professor position. This work has been partially supported by contract ANR-05-BLAN-0105-01 of the Agence Nationale de la Recherche in France.

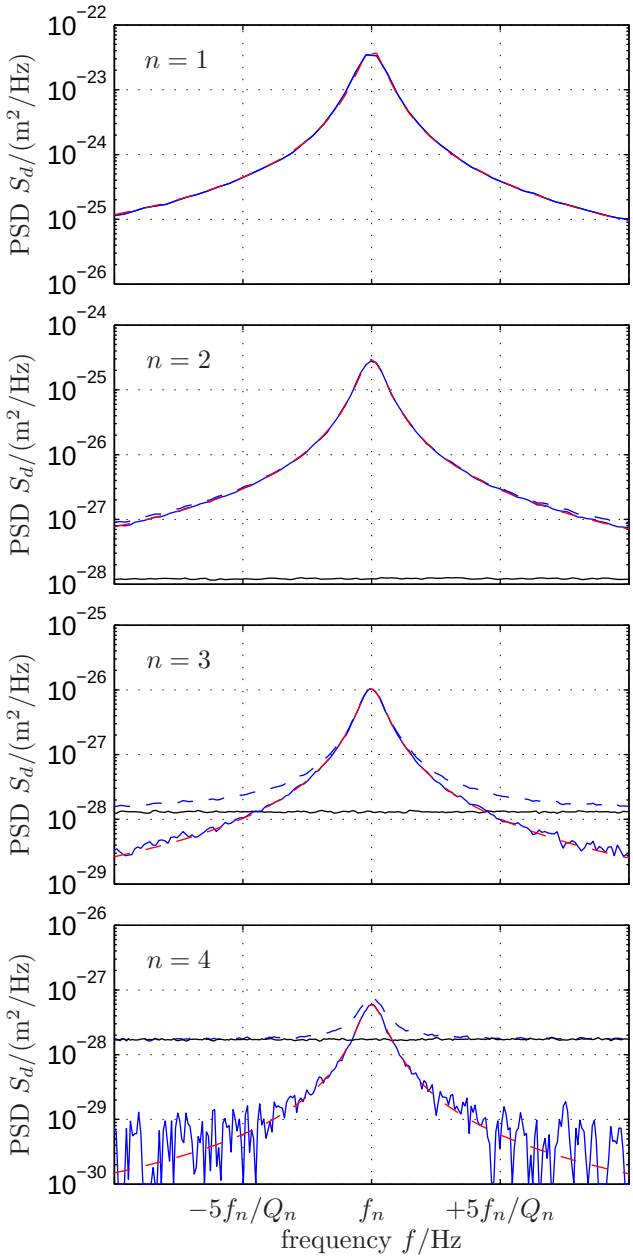

Figure 5: Power Spectrum Density (PSD) S_d of thermal noise induced deflexion measured close to the free end of the cantilever as a function of frequency f around each resonance f_n. We subtract from the raw measurement (dashed blue) the background noise (black) to estimate the mechanical noise of the cantilever (blue), then we perform a fit with a simple damped harmonic oscillator model (dashed red). For each plot, the horizontal scale spans $\pm 10 f_n/Q_n$ around f_n.

References

[1] H. J. Butt, B. Cappella, and M. Kappl. Force measurements with the atomic force microscope: Technique, interpretation and applications. *Surface Science Reports*, 59(1-6):1–152, 2005.

[2] Thomas E. Fisher, Piotr E. Marszalek, Andres F. Oberhauser, Mariano Carrion Vazquez, and Julio M. Fernandez. The micromechanics of single molecules studied with atomic force microscopy. *Journal of Physiology*, 520.1:5–14, 1999.

[3] Mariano Carrion Vazquez, Andres F. Oberhauser, Susan B. Fowler, Piotr E. Marszalek, Sheldon E. Broedel, Jane Clarke, and Julio M. Fernandez. Mechanical and chemical unfolding of a single protein: A comparison. *Proceedings of the National Academy of Sciences of the United States of America*, 96(7):3694–3699, 1999.

[4] P. Frederix, D. Bosshart, and A. Engel. Atomic force microscopy of biological membranes. *Biophys J*, 96:329–330, 2009.

[5] Manfred Radmacher. Studying the mechanics of cellular processes by atomic force microscopy. *Methods Cell Biol*, 83:347–372, 2007.

[6] F. Sbrana, C. Sassoli, E. Meacci, D. Nosi, R. Squecco, F. Paternostro, B. Tiribilli, S. Zecchi-Orlandini, F. Francini, and L. Formigli. Role for stress fiber contraction in surface tension development and stretch-activated channel regulation in c2c12 myoblasts. *American Journal of Physiology. Cell Physiology*, 295:160–172, 2008.

[7] Bharat Bhushan. Nanotribology, nanomechanics and nanomaterials characterization. *Philos Transact A Math Phys Eng Sci*, 366(1869):1351–1381, Apr 2008.

[8] Nickolay V. Lavrik, Michael J. Sepaniak, and Panos G. Datskos. Cantilever transducers as a platform for chemical and biological sensors. *Review of Scientific Instruments*, 75(7):2229–2253, 2004.

[9] S. M. Cook, T. E. Schaffer, K.M. Chynoweth, M. Wigton, R. W. Simmonds, and K. M. Lang. Practical implementation of dynamic methods for measuring atomic force microscope cantilever spring constants. *Nanotechnology*, 17:2135, 2006.

[10] R. Levy and M. Maaloum. Measuring the spring constant of atomic force microscope cantilevers: thermal fluctuations and other methods. *Nanotechnology*, 13:33, 2002.

[11] J. L. Hutter and J. Bechhoefer. Calibration of atomic-force microscope tips. *Review of Scientific Instruments*, 64(7):1868, 1993.

[12] John E. Sader, James W. M. Chon, and Paul Mulvaney. Calibration of rectangular atomic force microscope cantilevers. *Review of Scientific Instruments*, 70(10):3967–3969, 1999.

[13] N A Burnham, X Chen, C S Hodges, G A Matei, E J Thoreson, C J Roberts, M C Davies, and S J B Tendler. Comparison of calibration methods for atomic-force microscopy cantilevers. *Nanotechnology*, 14(1):1–6, 2003.

[14] H. J. Butt and M.Jaschke. Calculation of thermal noise in atomic force microscopy. *Nanotechnology*, 6:1, 1995.

[15] L. Bellon and P. Paolino. Procédé de mesure de la déflexion d'un levier de microscope à force atomique., 2008. Patent FR08/57952.

[16] P. Paolino and L. Bellon. Quadrature phase interferometer for afm measurement. *in preparation*, 2009.

[17] C. Schonenberger and S. F. Alvarado. A differential interferometer for force microscopy. *Review of Scientific Instruments*, 60(10):3131–3134, 1989.

[18] L. Bellon, S. Ciliberto, H. Boubaker, and L. Guyon. Differential interferometry with a complex contrast. *Opt. Comm.*, 207:49, 2002.

[19] J. E. Sader. Frequency response of cantilever beams immersed in viscous fluids with applications to the atomic force microscope. *Journal of Applied Physics*, 84(1):64, 1998.

[20] A. Maali, C. Hurth, R. Boisgard, C. Jai, T. Cohen-Bouhacina, and Jean-Pierre Aimé. Hydrodynamics of oscillating atomic force microscopy cantilevers in viscous fluids. *Journal of Applied Physics*, 97:074907, 2005.

[21] C. A. Van Eysden and J. E. Sader. Frequency response of cantilever beams immersed in viscous fluids with applications to the atomic force microscope: Arbitrary mode order. *Journal of Applied Physics*, 101:044908, 2007.